Surgical Neurology International

OPEN ACCESS

For entire Editorial Board visit : http://www.surgicalneurologyint.com

Editor: **James I. Ausman,** MD, PhD University of California, Los Angeles, CA, USA

Original Article

Classification of neurovascular compression in glossopharyngeal neuralgia: Three-dimensional visualization of the glossopharyngeal nerve

Levent Tanrikulu[1,2], Peter Hastreiter[1], Arnd Dörfler[3], Michael Buchfelder[1], Ramin Naraghi[1,4]

Departments of [1]Neurosurgery and [3]Neuroradiology, University of Erlangen-Nuremberg, Erlangen, [2]Department of Neurosurgery, Hannover Nordstadt Hospital, Hannover, [4]Department of Neurosurgery, Bundeswehrkrankenhaus Ulm, Ulm, Germany

E-mail: *Levent Tanrikulu - ltanrikulu@aol.de; Peter Hastreiter - Peter.hastreiter@uni-erlangen.de; Arnd Dörfler - Arnd.dorfler@uni-erlangen.de; Michael Buchfelder - Michael.buchfelder@uni-erlangen.de; Ramin Naraghi - Ramin-naraghi@t-online.de
*Corresponding author

Received: 25 August 15 Accepted: 08 October 15 Published: 24 December 15

Abstract

Background: We introduce a method of noninvasive topographical analysis of the neurovascular relationships of the glossopharyngeal nerve (CN IX) by three-dimensional (3D) visualization. Patients with glossopharyngeal neuralgia (GN) resulting from neurovascular compression (NVC) were studied.

Methods: 15 patients with GN were prospectively examined with 3D visualization using high-resolution magnetic resonance imaging with constructive interference in steady state (MR-CISS). The datasets were segmented and visualized with the real, individual neurovascular relationships by direct volume rendering. Segmentation and 3D visualization of the CN IX and corresponding blood vessels were performed. The 3D visualizations were interactively compared with the intraoperative setup during microvascular decompression (MVD) in order to verify the results by the observed surgical-anatomical findings.

Results: 15 patients (female/male: 5/10) were examined. All of them underwent MVD (100%). Microvascular details were documented. The posterior inferior cerebellar artery (PICA) was the most common causative vessel in 12 of 15 patients (80%), the vertebral artery (VA) alone in one case (6.7%), and the combination of compression by the VA and PICA in 3 patients (13.3%). We identified three distinct types of NVC within the root entry zone of CN IX.

Conclusion: 3D visualization by direct volume rendering of MR-CISS data offers the opportunity of noninvasive exploration and anatomical categorization of the CN IX. It proves to be advantageous in supporting to establish the diagnosis and microneurosurgical interventions by representing original, individual patient data in a 3D fashion. It provides an excellent global individual view over the entire neurovascular relationships of the brainstem and corresponding nerves in each case.

Key Words: Classification, glossopharyngeal nerve, glossopharyngeal neuralgia, image processing, neurovascular compression

Access this article online

Website: www.surgicalneurologyint.com

DOI: 10.4103/2152-7806.172534

Quick Response Code:

How to cite this article: Tanrikulu L, Hastreiter P, Dörfler A, Buchfelder M, Naraghi R. Classification of neurovascular compression in glossopharyngeal neuralgia: Three-dimensional visualization of the glossopharyngeal nerve. Surg Neurol Int 2015;6:189.
http://surgicalneurologyint.com/Classification-of-neurovascular-compression-in-glossopharyngeal-neuralgia:-Three-dimensional-visualization-of-the-glossopharyngeal-nerve/

INTRODUCTION

The glossopharyngeal nerve (CN IX) at the ventrolateral medulla oblongata features a complex formation in the posterior cranial fossa. The CN IX emerges from the retro-olivary sulcus in the region of the flower basket of Bochdalek and superiorly courses to the vagus nerve to the jugular foramen. At the root entry zone (REZ) of CN IX blood vessels such as the posterior inferior cerebellar artery (PICA) and the vertebral artery (VA) may compress the CN IX resulting in neurovascular compression (NVC).[10-12] This can lead to hyperexcitation and to clinical symptoms of glossopharyngeal neuralgia (GN), which is a very rare entity in comparison to trigeminal neuralgia and hemifacial spasm.[13] A pre- or intra-operative topographic global view over the microvascular relationships of the CN IX was difficult until now. The surgeon can only to see a limited portion of the neurovascular relationships during surgery. Image processing of this complex anatomical area has not been introduced as a routine. High-resolution magnetic resonance imaging (MRI) is the diagnostic method of choice for imaging of the CN IX. However, topographical differentiation and analysis of neurovascular relationships are difficult by two-dimensional (2D) representations based on image slices only. In this work, we applied the method of three-dimensional (3D) visualization of the CN IX and corresponding vessels to demonstrate neurovascular details for microsurgical planning. The results of 3D visualization were verified with the intraoperative documentation during the surgeries.

Table 1: Clinical data and results from 3D visualization and MVD

Patient No	Sex	Age	GN-Side	Vessel in 3D visualization	MVD	Postoperative pain result
1	m	54	Left	VA	+	Pain-free
2	m	55	Left	PICA	+	Pain-free
3	f	71	Left	PICA	+	Pain-free
4	f	67	Right	PICA	+	Pain-free
5	f	63	Left	PICA	+	Pain-free
6	m	58	Left	PICA	+	Pain-free
7	m	46	Left	PICA	+	Pain-free. Transient dysphagia
8	m	86	Right	PICA	+	Pain-free
9	m	55	Left	PICA	+	Pain-free
10	f	36	Right	PICA	+	Pain-free
11	m	49	Right	PICA	+	Pain-free
12	m	47	Right	PICA+VA	+	Pain-free
13	m	54	Left	PICA+VA	+	Pain-free
14	f	44	Left	PICA	+	Pain-reduction. Transient CSF leak
15	m	39	Left	PICA	+	Pain-free

No.: Number, GN: Glossopharyngeal neuralgia, 3D: Three-dimensional, MVD: Microvascular decompression, CSF: Cerebrospinal fluid

CLINICAL MATERIAL AND METHODS

Clinical data

We studied 15 patients with GN [Table 1]. All patients were treated by microvascular decompression (MVD) (100%). The diagnosis was made by clinical examination. Surgery consisted of MVD as described by Jannetta including intraoperative monitoring of brainstem auditory evoked potentials and vocal cord monitoring.[4,6-8] Intraoperative interactive 3D visualization was applied in each procedure.

Imaging

Imaging was performed with a Siemens MR Magnetom Sonata 1.5 Tesla scanner. MRI with constructive interference in steady state (MR-CISS) as highly T2-weighted sequence was used (Time of repetition/Time of echo (TR/TE) 12.2/5.9 ms, flip angle 70°, acquisition time 5 min, matrix 512 × 512, and slice thickness 0.4 mm).[8,11] Highly resoluted MRI and isotropic voxel sizes were applied for image postprocessing. MR-CISS delivers datasets in three dimensions with axial, coronal, and sagittal orientation. The MR-CISS sequence provides a high contrast between hyperintense cerebrospinal fluid (CSF) and hypointense cranial nerves and vessels [Figure 1]. This enables differentiation of tiny structures with a diameter of 0.4 mm. The pulsation of CSF within the lateral medulla oblongata where the CN IX emerges from the brainstem is low in contrast to the CSF pulsation within the midline area with the basilar artery.

Image processing

Image processing consists of segmentation and direct volume rendering. Segmentation consists of the coarse extraction of relevant structures [Figure 2a].[1,9] The CSF-space including the cranial nerves and vessels is segmented by volume growing and appears transparent while the vessels and nerves appear opaque using the information of the intensity of each voxel [Figure 2a].[1,9] The result of image processing is a real 3D presentation of the brainstem, vessels, and the cranial nerves. The examiner can view the resulting 3D object from any direction and is able to manipulate the position of the object interactively [Figure 2b]. We evaluated the possibility to visualize the detailed neurovascular conflicts in patients with GN to draw a classification of distinct types of NVC of the CN IX at the ventrolateral medulla oblongata.

RESULTS

The MR-CISS images clearly depicted the CN IXs and corresponding vessels within the hyperintense CSF volume. We could distinguish nerves from vessels on the basis of signal intensity, anatomical characteristics, and the anatomical course in the MR-CISS. The

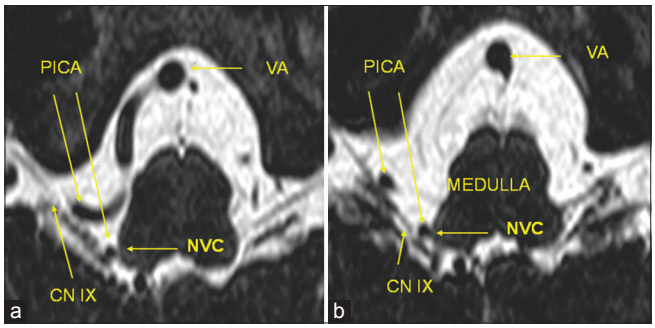

Figure 1: High-resolution magnetic resonance imaging with constructive interference in steady state sequence with neurovascular compression of the right-sided glossopharyngeal nerve. (a and b) A right-sided posterior inferior cerebellar artery-loop originating from the vertebral artery and coursing into the root entry zone of the glossopharyngeal nerve at the ventrolateral medulla oblongata. VA: Vertebral artery, PICA: Posterior inferior cerebellar artery, CN IX: Glossopharyngeal nerve, NVC: Neurov l ascular compression

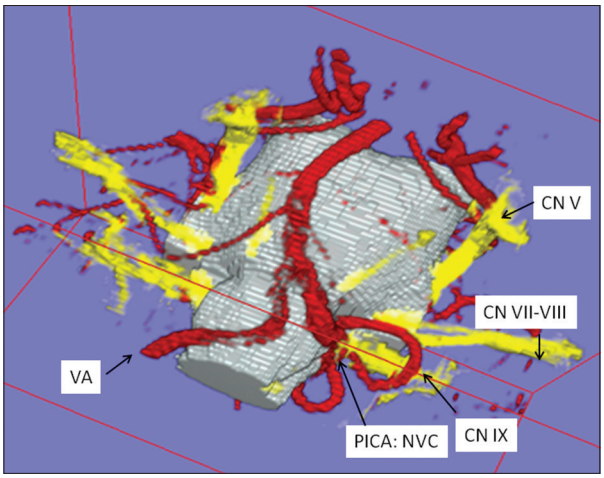

Figure 3: Three-dimensional visualization in left-sided glossopharyngeal neuralgia. A posterior inferior cerebellar artery-loop originating from the left vertebral artery courses over the left glossopharyngeal nerve and performs neurovascular compression at the glossopharyngeal root entry zone at the ventrolateral medulla oblongata (VA: Vertebral artery, PICA: Posterior inferior cerebellar artery, CN IX: Glossopharyngeal nerve)

interactive 3D visualization demonstrated the spatial relationships between the CN IX and the corresponding vessels in all patients (100%); [Figures 3 and 4]. The PICA was the most common causative vessel in 12 out of 15 patients (80%), the VA alone in one case (6.7%) and the combination of a compression by the VA and the PICA in two cases (13.3%). Each offending vessel at the REZ of CN IX, which was visualized preoperatively, could also be detected intraoperatively (Figures 3 and 6a-c; the operative field in Figures 6a-c correspond to the 3D visualization in Figure 3). The surgeon was able to observe the entire microvascular and neural structures within the CSF space of the individual patient by 3D visualization corresponding to the microsurgical operative domain. Pulsation artifacts were not observed

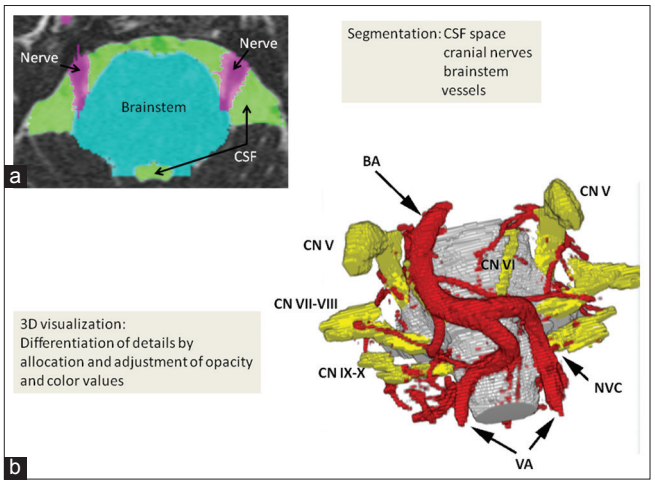

Figure 2: Workflow of image processing. (a) Segmentation of magnetic resonance imaging with constructive interference in steady state sequence: Each anatomical subvolume, cerebrospinal fluid space including vessels (green color), cranial nerves (purple color), and the brainstem (turquoise color) are segmented. (b) After segmentation of each subvolume, the acquired volumes are adjusted and allocated to opacity and color values, so that a real, individual three-dimensional representation based on the anatomical magnetic resonance imaging with constructive interference in steady state data is visualized. This three-dimensional visualization object can be rotated in each direction to observe the interesting topographical regions in a noninvasive way (BA: Basilar artery, VA: Vertebral artery, CN V: Trigeminal nerve, CN VI: Abducens nerve, CN VII-VIII: Facial-vestibulocochlear nerve, CN IX-X: Glossopharyngeal-vagus nerve)

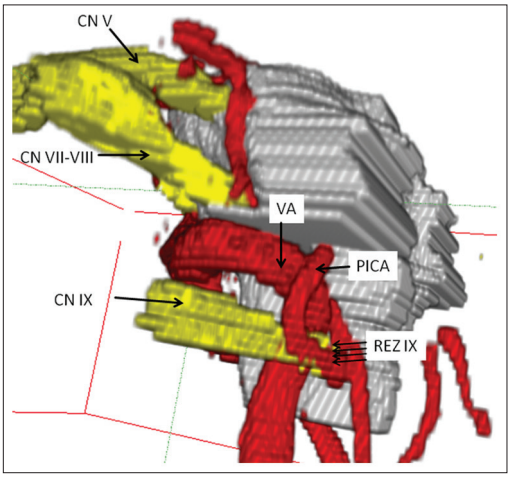

Figure 4: Lateral view of three-dimensional visualization in left-sided glossopharyngeal neuralgia. neurovascular compression is performed by a "sandwich" compression of the root entry zone of the glossopharyngeal nerve by the left-sided vertebral artery and a branching loop of posterior inferior cerebellar artery (CN IX: Glossopharyngeal nerve, REZ: Root entry zone, CN VII-VIII: Facial-vestibulocochlear nerve, CN V: Trigeminal nerve, VA: Vertebral artery, PICA: Posterior inferior cerebellar artery)

at the lateral medulla oblongata and the interesting CN IXs. We were able to find several characteristic situations which led us to describe distinct types of NVC [Figure 5]. The PICA, as coming from the VA has first

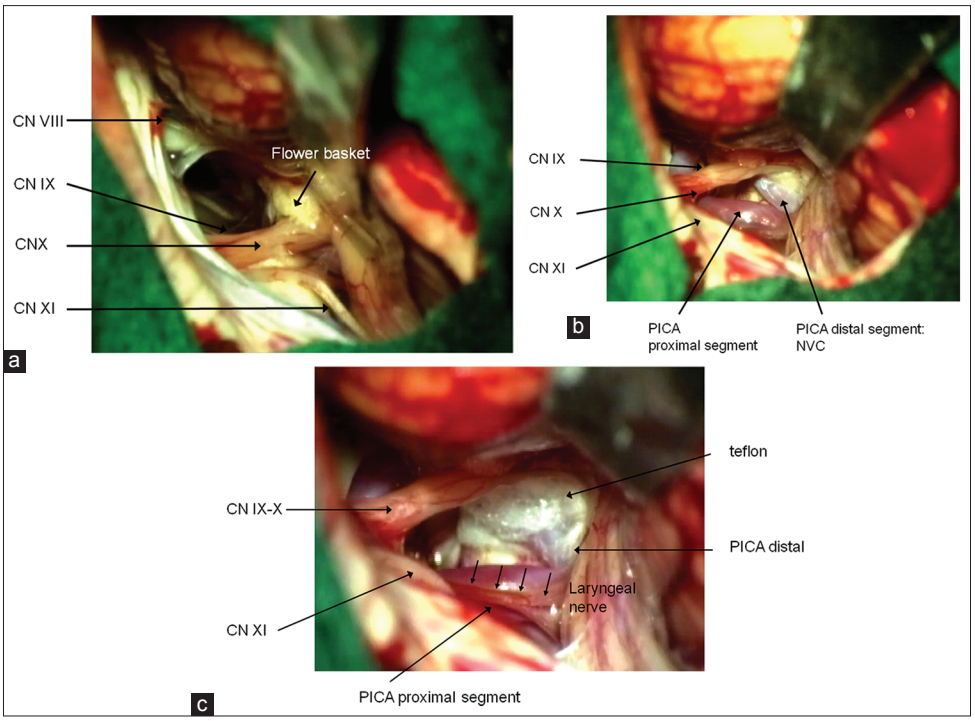

Figure 5: Types of neurovascular compression of the glossopharyngeal nerve. Type I as the most frequent one is caused by the posterior inferior cerebellar artery, which travels first cranially and performs neurovascular compression by a downward directed convex dome more distally. Type II is performed by the "shoulder" of the vertebral artery. Type III is performed by the combination of compression by the vertebral artery and the branching posterior inferior cerebellar artery

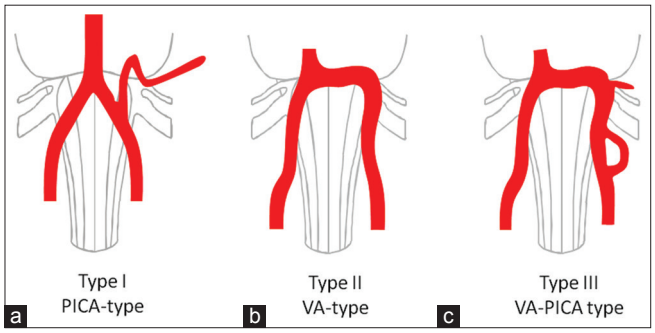

Figure 6: Surgical aspect of microvascular decompression by the interpolation of teflon between the nerve and the causative vessel. The surgical microphotographs correspond to three-dimensional visualization in Figure 3. (a) Microneurosurgical view over the anatomical findings in a patient with left-sided glossopharyngeal neuralgia after left-sided suboccipital, retrosigmoid craniectomy, release of cerebrospinal fluid from cisterna magna and cerebellar retraction (CN VIII: Vestibulocochlear nerve, CN IX: Glossopharyngeal nerve, CN X: Vagus nerve, CN XI: Accessory nerve). Note the clear view over Bochdalek's flower basket at the nerval interspace between the glossopharyngeal and the vagus nerves. (b) Preparation of the causative vessel: The posterior inferior cerebellar artery originates medially from the vertebral artery and performs a loop over the glossopharyngeal-vagus nerve complex with its proximal segment. More distally the posterior inferior cerebellar artery performs neurovascular compression at the glossopharyngeal root entry zone at the ventrolateral medulla oblongata by performing a downward complex dome. (c) Microvascular decompression with teflon. Note the visualization of the more caudally localized and preserved laryngeal nerve

to travel cranially and later downward after performing a loop over the IX-X-nerve-complex as proximal vessel portion and then performing NVC at the REZ of the CN IX within the retro-olivary sulcus and coursing more laterally [Figure 5, Type I]. The VA alone performs NVC at the glossopharyngeal REZ by the shoulder of the vessel [Figure 5, Type II]. A "sandwich-like" compression was observed in cases where the VA and the PICA perform a combination of compression [Figure 5, Type III].

Five patients showed right-sided neuralgia (33%) and 10 patients showed left-sided neuralgia (67%). In this series, 14 of 15 patients (93.3%) become pain-free in the postoperative period (follow-up 6–48 months), whereas 1 patient (6.7%) showed pain-reduction instead of pain-freedom. One patient showed transient dysphagia (6.7%), and another one showed transient CSF leak (6.7%; Table 1).

DISCUSSION

2D representations do not give sufficient information over the spatial relationships of nerves and vessels. Therefore, we introduced and applied the technique of direct volume rendering to obtain 3D visualization of the CN IX. For optimized imaging of the CN IX, the MR-CISS sequence was applied. This imaging sequence improved

the contrast between neighboring structures mostly allowing differentiation of nerves and vessels within the CSF space. Isotropic voxel sizes of the volume data were used to improve the interplane resolution. This ensured equal high-resolution in the axial, coronal, and sagittal slices. The lateral medulla oblongata containing the CN IXs is demonstrated very well in contrast to the cisternal compartiments around the midline. In the axial slice images of MR-CISS, we were able to differentiate the CN IXs, as well as all other remaining cranial nerves V-XI. In each case, we were able to visualize the CN IXs. Interactive 3D visualization is a prerequisite for comprehensive analysis and understanding of volumetric data from MRI. The segmentation of MR-CISS takes about 1–2 h, and the adjustment of transfer functions referring to direct volume rendering takes <3 min. The visualization of the neurovascular structures of the CN IX was useful in preoperative planning and during surgery. We applied the 3D visualization intraoperatively and analyzed microsurgical details during MVD. 3D visualization of neurovascular structures provides a great deal of topographic information before surgery. A classification of the vascular courses causing NVC in GN does not exist until now. This classification is considered to be necessary for a reproducible and standardized evaluation in establishing the diagnosis, planning, and performing surgery. The suggested classification derived from original individual data was able to cover all anatomical situations, which we found in this analysis. We did not find any tumorous mass within the surface of the lateral medulla oblongata neither in the preoperative, diagnostic MRI nor during surgery, which could also be another possible cause of GN.[7,8]

We can confirm that MVD is the treatment of choice for medication-refractory GN.[3,8] GN is a very rare condition[2,3] and we think that – although our series might not be very large – the high rate of success even as long-term can be attributed to the method of 3D visualization introduced here. We consequently applied the MR-CISS sequences for the segmentation and 3D visualization. Of course MR-angiography (time of flight) can additionally be used in addition to the MR-CISS sequences for the detection of NVC in the posterior fossa such as reported by Leal *et al*.[5]

CONCLUSIONS

We presented a method of noninvasive evaluation of the relationships of the CN IX and the corresponding blood vessels with high-resolution MRI using MR-CISS and 3D visualization based on direct volume rendering in patients with GN. Distinct types of courses of vessels causing NVC are described. Several characteristics for the identification of NVC were described allowing a reproducible and standardized evaluation of the neurovascular relationships. We suggest this method of noninvasive anatomical exploration of the CN IX as very useful for topographic classification of the variable vascular compression courses along the REZ of the CN IX in order to support diagnostic and surgical procedures.

Financial support and sponsorship
Nil.

Conflicts of interest
There are no conflicts of interest.

REFERENCES

1. Hastreiter P, Naraghi R, Tomandl B, Bonk A, Fahlbusch R. Analysis and 3-dimensional visualization of neurovascular compression syndromes. Acad Radiol 2003;10:1369-79.
2. Headache Classification Subcommittee of the International Headache Society. The international classification of headache disorders: 2nd edition. Cephalalgia 2004;24 Suppl 1:9-160.
3. Jannetta PJ, Segal R, Wolfson SK Jr, Dujovny M, Semba A, Cook EE. Neurogenic hypertension: Etiology and surgical treatment. II. Observations in an experimental nonhuman primate model. Ann Surg 1985;202:253-61.
4. Kalkanis SN, Eskandar EN, Carter BS, Barker FG 2nd. Microvascular decompression surgery in the United States, 1996 to 2000: Mortality rates, morbidity rates, and the effects of hospital and surgeon volumes. Neurosurgery 2003;52:1251-61.
5. Leal PR, Hermier M, Froment JC, Souza MA, Cristino-Filho G, Sindou M. Preoperative demonstration of the neurovascular compression characteristics with special emphasis on the degree of compression, using high-resolution magnetic resonance imaging: A prospective study, with comparison to surgical findings, in 100 consecutive patients who underwent microvascular decompression for trigeminal neuralgia. Acta Neurochir (Wien) 2010;152:817-25.
6. Levy EI, Scarrow AM, Jannetta PJ. Microvascular decompression in the treatment of hypertension: Review and update. Surg Neurol 2001;55:2-10.
7. Marion DW, Jannetta PJ. Use of perioperative steroids with microvascular decompression operations. Neurosurgery 1988;22:353-7.
8. McLaughlin MR, Jannetta PJ, Clyde BL, Subach BR, Comey CH, Resnick DK. Microvascular decompression of cranial nerves: Lessons learned after 4400 operations. J Neurosurg 1999;90:1-8.
9. Naraghi R, Hastreiter P, Tomandl B, Bonk A, Huk W, Fahlbusch R. Three-dimensional visualization of neurovascular relationships in the posterior fossa: Technique and clinical application. J Neurosurg 2004;100:1025-35.
10. Resnick DK, Jannetta PJ, Bissonnette D, Jho HD, Lanzino G. Microvascular decompression for glossopharyngeal neuralgia. Neurosurgery 1995;36:64-8.
11. Rozen TD. Trigeminal neuralgia and glossopharyngeal neuralgia. Neurol Clin 2004;22:185-206.
12. Rushton JG, Stevens JC, Miller RH. Glossopharyngeal (vagoglossopharyngeal) neuralgia: A study of 217 cases. Arch Neurol 1981;38:201-5.
13. Sampson JH, Grossi PM, Asaoka K, Fukushima T. Microvascular decompression for glossopharyngeal neuralgia: Long-term effectiveness and complication avoidance. Neurosurgery 2004;54:884-9.